FACTA UNIVERSITATIS
Series: **Mechanics, Automatic Control and Robotics** Vol.3, N° 13, 2003, pp. 739 - 744

MICROSCOPIC OBSERVATION OF FIBER DEFORMATION AND FRACTURE DURING MACHINING OF A-FRP

UDC 539.388.2

Eitoku Nakanishi, Yutaka Sawaki, Kiyoshi Isogimi

Department of Mechanical Engineering, Faculty of Engineering, Mie University
Kamihama 1515, Tsu. 514-8507, Japan
E-mail: isogami@mach.mie-u.ac.jp

Abstracts. *We observed the deformation and fractural phenomena of Aramid fiber during machining of A-FRP by microscopically. We can make deformation and fracture of fiber clear that is situated in the matrix in transmittal. When the fiber angle θ is 45 degree, Aramid fibers are strongly pressed and expanded widely towards the cutting direction and peel off under the machined surface during a cutting tool passes. After the tool passed, a deformed fiber remains as a fluff. Further, we simulated the phenomena with a very simple model to evaluate the deformation of fiber during machining. It is based on S.P. Timoshenko's theory of beams on elastic foundation. In our analysis, the modulus of the foundation is varied to prove the orientation of fiber. The calculated results have some coincides with experimental results.*

EXPERIMENTAL METHOD

We observed the deformation and fractural phenomena of Aramid fiber during machining of A-FRP by microscopically. WC cutting tool was chosen and two kinds of specimen were employed as shown in Fig.1. Each specimen contains only one bundle of Aramid fibers in two kinds of orientations and the matrix is polyester. Figure2 shows the experimental equipment. The cutting speed was 10mm/min and the cutting depth was 0.05 mm. A micrometer controlled the cutting depth. Dynamic cutting phenomena was observed by CCD camera through a microscope and recorded by a personal computer.

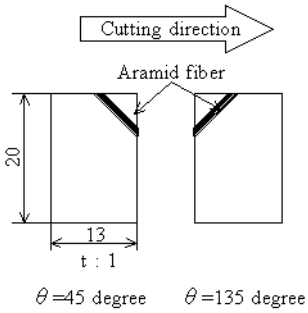

Fig. 1. A-FRP specimen

Received October 20, 2002

EXPERIMENTAL RESULTS

Figure 3 and 4 show the machining process of A-FRP. When the fiber angle θ is 45 degree, the tool face touches the Aramid fiber firstly and then cutting edge touches the fiber. In this case, it becomes difficult for cutting edge to cut the fiber well. And Aramid fibers are lifted up by a tool face and elongated towards cutting direction during machining. Further the Aramid fibers are deformed from the inside of matrix and peel off under the machined surface. The depth of the peeling off became about same as cutting depth. After the tool passed, higher fluffs remains on machined surface. Due to the presence of the fluffs, the surface integrities of machined surface became poor. On the other hand, when fiber angle θ is 135 degree, the cutting edge touches the Aramid fiber firstly and cuts the fiber well. Fiber deforms in a very small region and is not lifted up by tool edge. And after the tool passed, the fluffs hardly appear on machined surface.

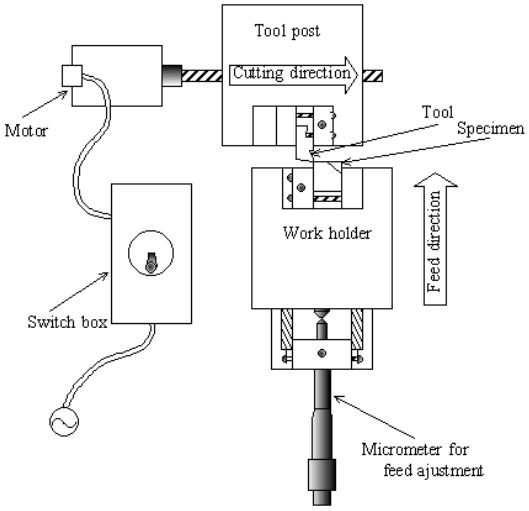

Fig. 2. Experimental setup

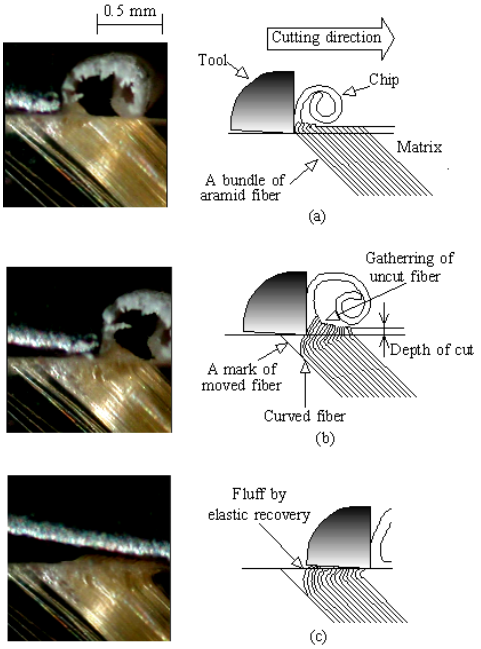

Fig. 3. Dynamic cutting process in fiber angle θ = 45 degree

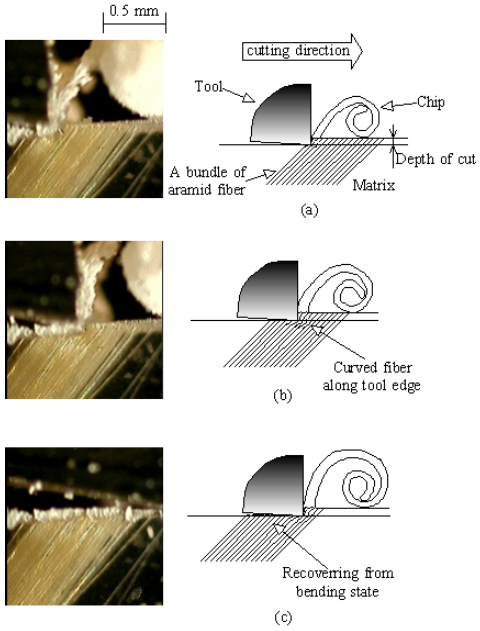

Fig. 4. Dynamic cutting process in fiber angle θ =135 degree

MODELING

We made a simple model for evaluate the Aramid fiber deformation during machining that is based on S.P. Timoshenko's theory of beams on elastic foundation [1] and Dr.WANG's theory [2]. In the analysis, two modes of tool-fiber contact are considered for each fiber orientations as shown in Fig.5. In Fig. 5, the value d is a cutting depth and is 0.05mm. And the beams are regarded as Aramid fibers and the elastic foundation is regarded as matrix material as shown in Fig. 6. By this calculation, we can evaluate the deformation of Aramid fiber for each orientation during machining as value Y. When fiber angle θ is 45 degree, tool face touches the end of fiber firstly. When fiber angle θ is 135 degree, cutting edge touches at the distant of u (= d/sin θ) from end of the fiber firstly. In this analysis, the cutting force are regarded as two ways, moment M_0 and M_1 and normal force to fiber P and Q, respectively. These values are derived from our previous experimental results [3], as $P = 8.47$(N), $Q = 48.1$(N), $M_0 = 2.41\times10^{-4}$(Nm) and $M_1 = -4.2\times10^{-5}$(Nm), respectively.

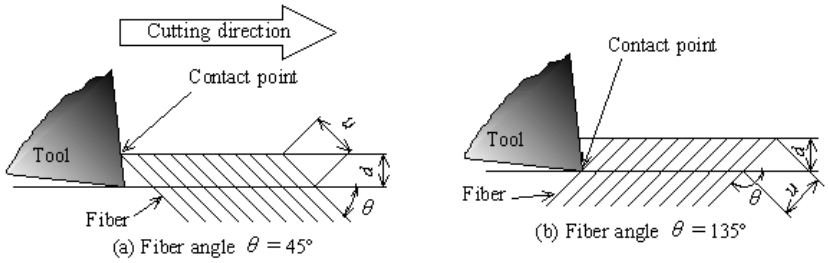

Fig. 5. Two modes of tool-fiber contact

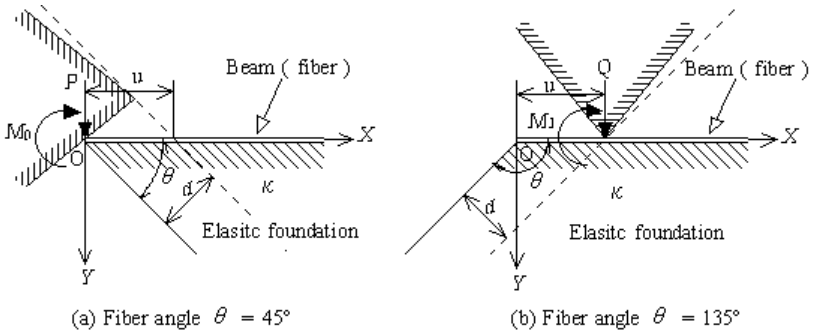

Fig. 6. Two models as a half infinite beam on elastic foundation

Equation 1 is for fiber angle θ = 45 degree and Eq.2 is for fiber angle θ = 35 degree. Where, I_z is geometry moment of intertia for Aramid fiber, r_f is a radius of Aramid fiber and E_f is young's modulus of Aramid fiber, respectively.

Dr. WANG applied this theory for machining G-FRP. As well known, glass fiber is very brittle and Aramid fiber is not brittle and deforms much during machining, so some improvement was required. We varied the value k (Unit reaction force for unit strain, N/mm^2) along the Aramid fiber. When fiber angle θ = 45 degree, near the machined

surface, the tool edge lifts up the Aramid fiber and loses the support of matrix. It is considered the value k increases linearly with X as shown in Eq.3. Equation 3 indicates that reaction force of matrix is weak near the machined surface and at deeper location it becomes strong. In this paper, k is approximated as follows, at the end of fiber (Point O, $X = 0$) $k = k_E = 12\times10^7$, at $0 < X < g$ k increases linearly with X, at $g < X$ $k = k_d = 550\times10^7$. And the value g is a length of peeling of between matrix and Aramid fiber and is assumed to be 5.6×10^{-4} (m) from experimental result.

$$Y = \frac{\exp(-\beta X)[P\cos\beta X - \beta M_o(\cos\beta X - \sin\beta X)]}{2\beta^3 E_f I_z} \tag{1}$$

where,

$$\beta = \sqrt[4]{\frac{k}{4E_f I_z}}\ \text{(1/m)},\quad I_z = \frac{\pi r_f{}^4}{4}\ (\text{m}^4),\quad r_f = 6\times10^{-5}\,(\text{mm}),\quad E_f = 107.8\times10^9\,(\text{Pa})$$

$$Y = Y' + Y'' \tag{2}$$

where,

$$Y' = \frac{Q\beta}{2k}\varphi(\beta X) + \frac{Q\beta}{k}\left\{\rho(\beta u)\rho[\beta(X+u)] + \frac{1}{2}\psi(\beta u)\rho[\beta(X+u)] - \frac{1}{2}\psi(\beta u)\zeta[\beta(X+u)]\right\}$$

$$Y'' = \frac{M_1\beta^2}{k}\zeta(\beta X) + \frac{M_1\beta^2}{k}\rho(\beta u)\varphi[\beta(X+u)] + \frac{M_1\beta^2}{2k}\psi(\beta u)\varphi[\beta(X+u)] + \frac{M_1\beta^2}{2k}\psi(\beta u)\psi[\beta(X+u)]$$

$$\begin{aligned}
&\varphi(\beta X) = \exp(-\beta X)(\cos\beta X + \sin\beta X) && \varphi(\beta u) = \varphi(\beta X)_{X=u}\\
&\psi(\beta X) = -\exp(-\beta X)(\sin\beta X - \cos\beta X) && \psi(\beta u) = \psi(\beta X)_{X=u}\\
&\rho(\beta X) = \exp(-\beta X)\cos\beta X && \rho(\beta u) = \rho(\beta X)_{X=u}\\
&\zeta(\beta X) = \exp(-\beta X)\sin\beta X && \zeta(\beta u) = \zeta(\beta X)_{X=u}
\end{aligned}$$

$$k = k_E + \frac{k_d - k_E}{g}X \tag{3}$$

Figure 7 shows the calculation results for deformation of the fibers during machining. When fiber angle θ is 45 degree, we can find large deformation at point O (end of fiber) and value Y (deformation) decreases with X (distance from machined surface along Aramid fiber). And it can be thought that with advancing of machining, it keeps a large deformation at point O and fiber can not be cut smoothly because cutting force is not concentrated at a contact point of cutting edge and Aramid fiber. On the other hand, when fiber angle θ is 135 degree we can find a deformation just at a contact point of cutting edge and Aramid fiber (point O). And it can be thought that the cutting force is concentrated at this point, so the fiber can be cut easily. And longer fluffs hardly appear on machined surface in this case θ = 135 degree.

CONCLUSIONS

We could observe the Aramid fiber deformation during machining in microscopically. Especially, when fiber angle θ is 45 degree, a peeling off at fiber-matrix interface and large

deformation of Aramid fiber inside of matrix could be observed clearly. Further, We could simulate the deformation of fiber during machining with a very simple method. By varying the value k (Unit reaction force for unit strain), the calculated results showed the good coincides with experimental results for each fiber orientations of A-FRP specimens.

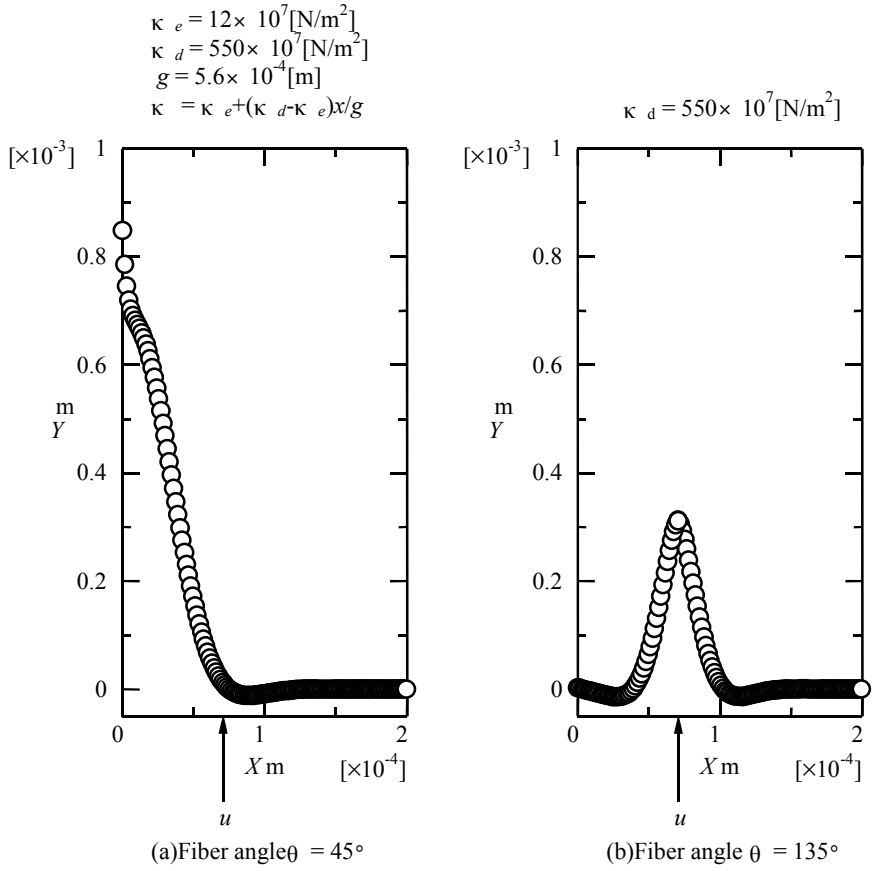

Fig. 7. Deformation in two models

REFERENCES

1. S. Timoshenko, (1930), Strength of Material, Part2 Advanced Theory and Problems, D. Van Nostrand Co. Inc., pp.408.
2. Xiaodu Wang, Kazuo Nakayama and Minoru Arai, (1991), Investigation on the Cutting Fiber Reinforced Composite Materials (2nd Report), JSPE, Vol.57, No.8, pp. 129-134.
3. Nakanishi E, Isogimi K, (2000), The Fracture Mechanism of A-FRP during Cutting, Proc. of SEM, I.C.E.M., pp.233-236.

MIKROSKOPSKO POSMATRANJE DEFORMACIJE I LOMA VLAKNA TOKOM MAŠINSKE OBRADE A-FRP

Eitoku Nakanishi, Yutaka Sawaki, Kiyoshi Isogimi

Mikroskopski smo posmatrali pojave deformacije i loma Aramid vlakna tokom mašinske obrade A-FRP. Jasna je ona deformacija i lom vlakna koja je smeštena u matricu u prenosu. Kada je ugao vlakna 45 stepeni, Aramid vlakna su snažno pritisnuta i široko rastegnuta u smeru sečenja, i ljušte se pod mašinskom površinom prilikom prelaska alatke za sečenje. Nakon prolaska alatke, deformisano vlakno postaje paperjasto. Pored toga, simulirali smo pojave pomoću veoma jednostavnog modela da bismo procenili deformaciju vlakna tokom mašinske obrade. On je zasnovan na S.P. Timosenkovoj teoriji poluga na elastičnom postolju. U našoj analizi, modul postolja menja se da bi se dokazalo usmerenje vlakana. Izračunati rezultati se u nekim slučajevima podudaraju sa sa eksperimentalnim rezultatima.